

unlike GraphDRP and XGDP, tCNN used 1D convolutional layers to encode the SMILES notation of drugs, which renders it infeasible to decode the developed models to investigate structural saliency of drugs upon reaction with cancer cells.

Blind prediction of responses of unknown drugs

In the blind test of response prediction of unknown drugs, we divide the dataset by constraining the existence of drugs exclusively in training, validation, or testing set. Specifically, out of 223 drugs in total, 167 drugs' response data are used for a 3-fold cross-validation, and response data of 56 drugs are preserved for testing. The blind prediction task aims at testing whether the model developed on known drugs has the generalizability to predict responses of unknown drugs.

In the blind test experiment, we compare our method with tCNN, GraphDRP and TGSA. DeepCDR is ignored since the code to flexibly divide the dataset according to drug occurrence is not provided. As shown in Table 2, GAT- and GAT_E-based XGDP remarkably outperform other models. All baseline methods fail to perform well on blind test, especially in terms of R^2 , which is in accordance with their original research^{11,25,27}. tCNN and TGSA achieves a very small R^2 value (~ 0.02) and GraphDRP even results in negative R^2 values, which indicates these models are not making a sensible prediction when a brand new drug is given. Nevertheless, GAT-based XGDP models with and without edge features are able to achieve a significant improvement compared with the baselines.

XGDP achieves state-of-the-art performance in both rediscovery and blind test. However, scrutinizing the results of XGDP with various GNN types, it is observed that incorporating chemical bond type as edge features or relation types in relational GNNs does not always give rise to a better performance. Despite that RGCN outperforms GCN in both tasks, GAT-based XGDP suppresses all other edge-enhanced GAT models in Table 1, and in Table 2, only GAT_E performs better than plain GAT convolution. Nonetheless, in the next section, we will demonstrate that, to investigate the structural importance of molecules, it is essential to include edge features as well.

Prediction without cross-attention layers

To investigate the role of the cross-attention layers, we conducted an ablation study to compare XGDP with or without the attention layers. Particularly, we removed the two cross-attention modules following the GNN and CNN, and directly concatenated the features learned by the GNN and CNN modules as the input of the final dense layer. As shown in Table 3, it is evident that the cross-attention layer enhances the performance of drug response prediction and maintains better stability.

Discovery of drug mechanisms

We decode our models with GNNExplainer and Integrated Gradients, and present the attribution results of our best performing GATv2 model in this section. GNNExplainer is leveraged to explain the model's graph convolutional layers, and thus attribute the input molecular graphs. By interpreting a reaction pair of drug and cell line, each node and edge in the molecular graph is assigned with a saliency score. For each drug, we sum and average the saliency scores across all the cell lines for each node and edge, and perform a max-min normalization across the nodes or edges in one molecular graph. The normalized scores range from 0 to 1 and clearly illustrate the importance of a region of substructures to a drug's biochemical reaction. The normalized score is thereby used for a heatmap visualization, where red in Figs. 2, 3, 4, and 5 represents high saliency and blue represents low saliency.

To investigate the gene saliency in the pharmacodynamic process, we aggregate the saliency scores across all the cell lines for each drug in the test set, and thereby rank and select the top 50 genes with highest accumulated scores. Attribution of four drugs are illustrated as examples to support this study in the following sections.

Method	Conv type	RMSE (\downarrow)	PCC (\uparrow)	R^2 (\uparrow)
tCNN ¹¹	CNN	0.056 \pm 0.001	0.356 \pm 0.019	0.027 \pm 0.010
GraphDRP ²⁵	GCN	0.063 \pm 0.002	0.450 \pm 0.026	0.153 \pm 0.048
	GAT	0.071 \pm 0.003	0.351 \pm 0.165	-0.041 \pm 0.045
TGSA (exp) ²⁷	GraphSAGE	2.809 \pm 0.035	0.329 \pm 0.058	0.026 \pm 0.078
XGDP	GCN	0.056 \pm 0.000	0.400 \pm 0.016	0.048 \pm 0.015
	GAT	0.053 \pm 0.001	0.448 \pm 0.036	0.149 \pm 0.052
	GAT_E	0.052 \pm 0.003	0.505 \pm 0.090	0.164 \pm 0.043
	GATv2_E	0.055 \pm 0.002	0.442 \pm 0.041	0.058 \pm 0.024
	RGCN	0.055 \pm 0.001	0.405 \pm 0.031	0.063 \pm 0.045
	RGAT	0.055 \pm 0.002	0.257 \pm 0.061	0.063 \pm 0.060

Table 2. Performance of proposed and baseline models in task of drug-blind prediction. Best performance (marked in bold) is achieved by XGDP-GAT_E.

Method	Conv type	RMSE (↓)	PCC (↑)	R ² (↑)
XGDP (w/o attn)	GCN	0.045 ± 0.018	0.457 ± 0.476	0.480 ± 0.416
	GAT	0.038 ± 0.000	0.831 ± 0.003	0.679 ± 0.000
	GAT_E	0.037 ± 0.001	0.834 ± 0.010	0.691 ± 0.020
	GATv2_E	0.035 ± 0.000	0.847 ± 0.001	0.718 ± 0.002
XGDP	GCN	0.026 ± 0.000	0.918 ± 0.001	0.843 ± 0.002
	GAT	0.026 ± 0.000	0.923 ± 0.000	0.851 ± 0.001
	GAT_E	0.026 ± 0.000	0.922 ± 0.001	0.849 ± 0.001
	GATv2_E	0.026 ± 0.000	0.921 ± 0.001	0.846 ± 0.001

Table 3. Performance of proposed and baseline models in task of drug-blind prediction. Best performance (marked in bold) is achieved by XGDP-GAT_E.

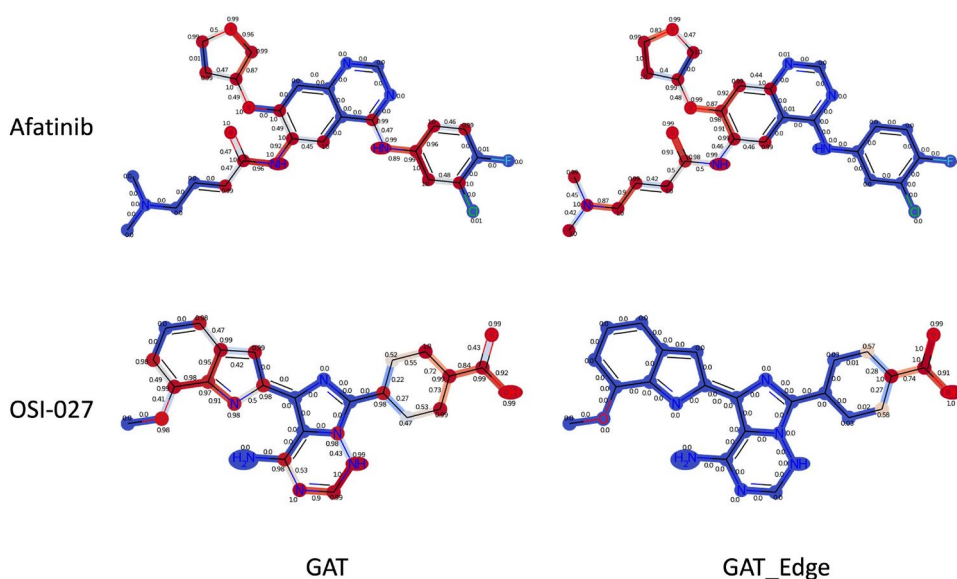


Fig. 3. Comparison of saliency maps generated by XGDP with GAT (left column) and GAT_E (right column). Afatinib (first row) and OSI-027 (second row) are used as examples.

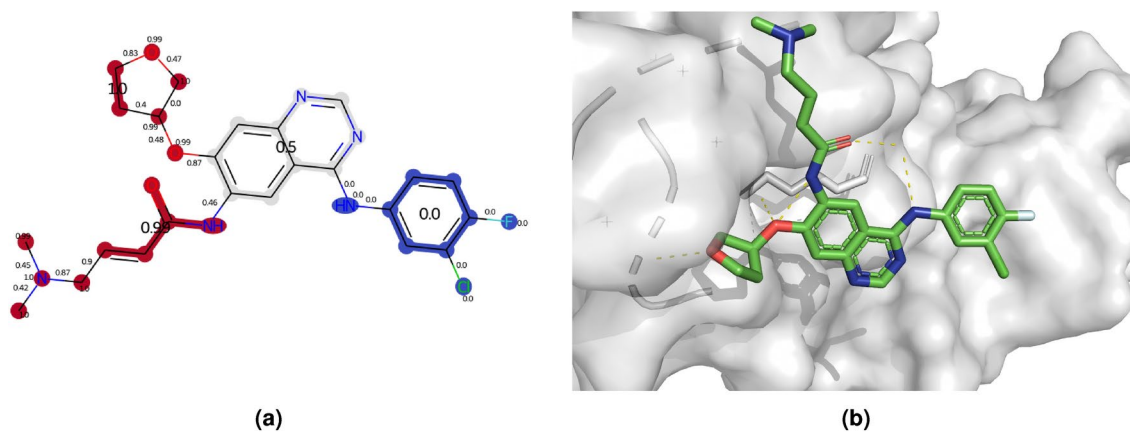


Fig. 4. (a) Saliency map of Afatinib, (b) binding mode of Afatinib with EGFR.

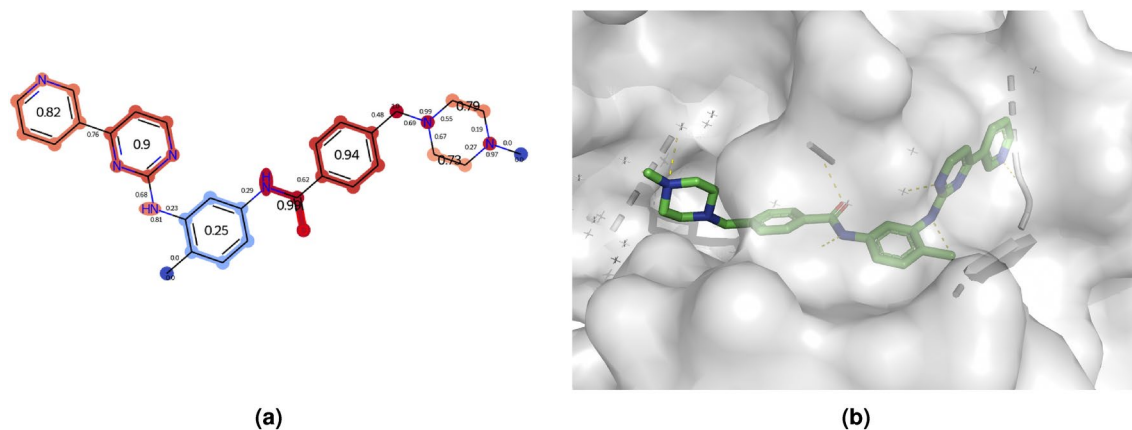


Fig. 5. (a) Saliency map of Imatinib, (b) binding mode of Imatinib with DDR1.

Necessity of including edge features

In the section of drug response prediction, we demonstrate that GAT-based XGDP obtained the best performance in both rediscovery and blind test. However, we do not observe any benefits of incorporating edge features such as bond types into model development. In this section, we will compare the molecular saliency heatmap obtained by interpreting GAT-XGDP with and without edge features.

Figure 3 presents the saliency maps generated by interpreting XGDP based on GAT and GAT_E. We observe that when edge features are absent in GAT convolutions, the model is likely to assign inconsistent saliency scores to atoms and bonds that are connected. Specifically, the case of atom with a high positive score and bond with a low negative score attached to the atom happens regularly in GAT-based models. This phenomenon thus hinders the study of substructure importance, since attached atom and bond are assigned with highly contrary saliency scores. However, this problem is overcome by GAT_E-based XGDP which incorporates edge features in model training. In the right column of Fig. 3, the significant (red) and insignificant (blue) structures are separated clearly instead of mixed with each other. Therefore, we conclude that edge features are essential for the model to correctly identify salient structures in molecules. The model decoding experiments in the following sections will all be conducted on XGDP-GAT_E model developed in the rediscovery test.

Chemical structure investigation

In this section, we took three drugs, i.e., Afatinib, Imatinib and Sunitinib, as examples to illustrate XGDP's capability of capturing salient substructures in drug reactions. We show the saliency heatmap of each drug and its binding mode with the protein target from the Protein Data Bank (PDB)⁵⁴. For a clearer illustration, we leveraged the Extended Functional Groups (EFG) algorithm⁵⁵ to identify the common functional groups in our dataset, and calculated the average of the saliency score of each atom in the functional group to present the importance of each functional group in the drug molecules. In the illustrations of drug protein binding mode, we show the contacts between drug molecule and its surroundings ($<5\text{\AA}$).

Afatinib is a famous EGFR inhibitor. According to⁵⁶, the acrylamide group in Afatinib is important for its inhibition to kinase activity of the ErbB family of proteins. As shown in Fig. 4, this functional group and other binding sites of Afatinib are successfully identified by our model. Imatinib is a DDR1 inhibitor. In Fig. 5, important binding sites, corresponding to the crystal structure of the DDR1 kinase in complex with Imatinib⁵⁷, such as the aminopyrimidine group, are assigned with a relatively high saliency score (> 0.9). Sunitinib is a potent PDGFR inhibitor⁵⁸. In the crystal structure of PDGFR in complex with Sunitinib (6JOK), the binding sites have been remarkably identified by our model as shown in Fig. 6.

Biomarker and pathway analysis

Table 4 presents the top genes (ranking < 200 in 956 genes) identified by XGDP that are recorded to have interactions with the corresponding drugs in the drug-gene interaction database⁵⁹. Particularly, ERBB3 and EGFR are ranked 60 and 78, respectively, out of 956 genes for Afatinib, DDR1 is ranked 16 for Imatinib, and PDGFA is ranked 113 for Sunitinib. Their specific interactions can be viewed in Figs. 3, 4, and 5.

Moreover, we perform Gene Set Enrichment Analysis (GSEA)⁶⁰ with GSEAPy⁶¹ using the attributed saliency scores. The top 5 enriched terms for each of the example drugs are shown in Table 5 together with their enrichment scores (ES) and normalized enrichment scores (NES). The identified pathways are well associated with cancer metastasis and progression. Specifically, epithelial-to-mesenchymal transition (EMT), which is one of the top enriched pathway for all drugs, is responsible for induction of cancer stem cells and immune escape during cancer progression in various cancers such as head and neck squamous-cell carcinoma (HNSC). Upregulation of KRAS signaling, which is usually the second most enriched pathway, is also found to be associated with a number of types of cancers such as breast cancer and pancreatic cancer. Therefore, we claim that the proposed method has the capability of capturing drug reaction mechanism and thus generating trustworthy prediction of drug responses.

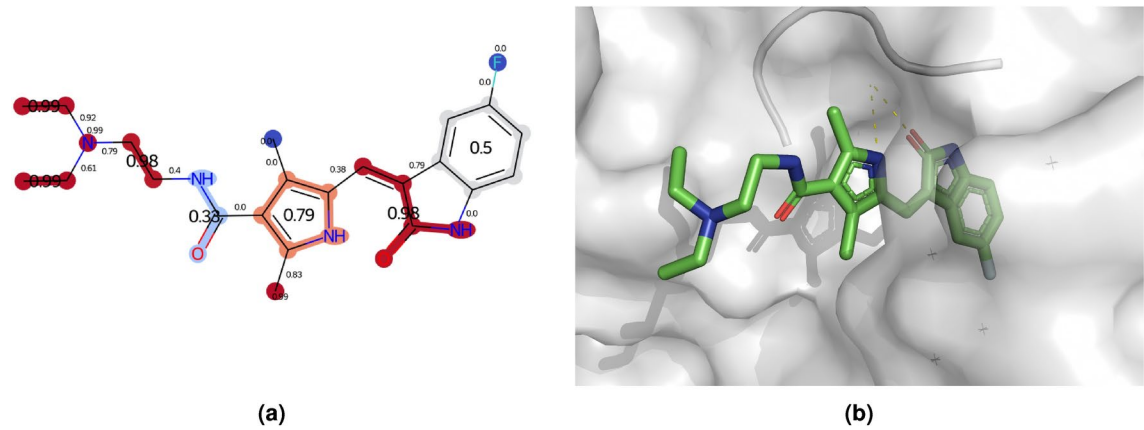


Fig. 6. (a) Saliency map of Sunitinib, (b) binding mode of Sunitinib with PDGFRA.

Drug	Gene	Rank	Saliency score
Afatinib	ERBB3	60	0.29
Afatinib	EGFR	78	0.26
Afatinib	ERBB2	108	0.23
Imatinib	MYC	2	0.85
Imatinib	SFN	10	0.64
Imatinib	DDR1	16	0.56
Imatinib	CDKN2A	23	0.54
Imatinib	EGFR	31	0.47
Imatinib	IKZF1	93	0.28
Imatinib	SMAD3	166	0.22
Sunitinib	NOS3	7	0.7
Sunitinib	EGFR	19	0.51
Sunitinib	FGFR2	47	0.36
Sunitinib	HMOX1	76	0.3
Sunitinib	PDGFA	113	0.27
Sunitinib	ERBB2	198	0.19

Table 4. Top salient genes identified by XGDP when predicting drug responses for Dasatinib, Erlotinib and Ponatinib.

Drug	Term	ES	NES
Afatinib	HALLMARK_KRAS_SIGNALING_UP	356.8	0.7
	HALLMARK_EPITHELIAL_MESENCHYMAL_TRANSITION	350.5	0.68
	HALLMARK_INFLAMMATORY_RESPONSE	316.08	0.62
	HALLMARK_ALLOGRAFT_REJECTION	268.76	0.52
	HALLMARK_APICAL_JUNCTION	268.5	0.52
Imatinib	HALLMARK_EPITHELIAL_MESENCHYMAL_TRANSITION	343.83	0.73
	HALLMARK_KRAS_SIGNALING_UP	298.37	0.63
	HALLMARK_APICAL_JUNCTION	289.58	0.62
	HALLMARK_MYOGENESIS	282.84	0.6
	HALLMARK_TNFA_SIGNALING_VIA_NFKB	280.9	0.6
Sunitinib	HALLMARK_EPITHELIAL_MESENCHYMAL_TRANSITION	345.81	0.73
	HALLMARK_KRAS_SIGNALING_UP	307.34	0.65
	HALLMARK_APICAL_JUNCTION	290.69	0.61
	HALLMARK_TNFA_SIGNALING_VIA_NFKB	277.54	0.59
	HALLMARK_UV_RESPONSE_DN	264.91	0.56

Table 5. Enriched pathways from GSEA on attributed saliency scores.